Report

Current Biology

# Brassinosteroids Dominate Hormonal Regulation of Plant Thermomorphogenesis via BZR1

## Graphical Abstract

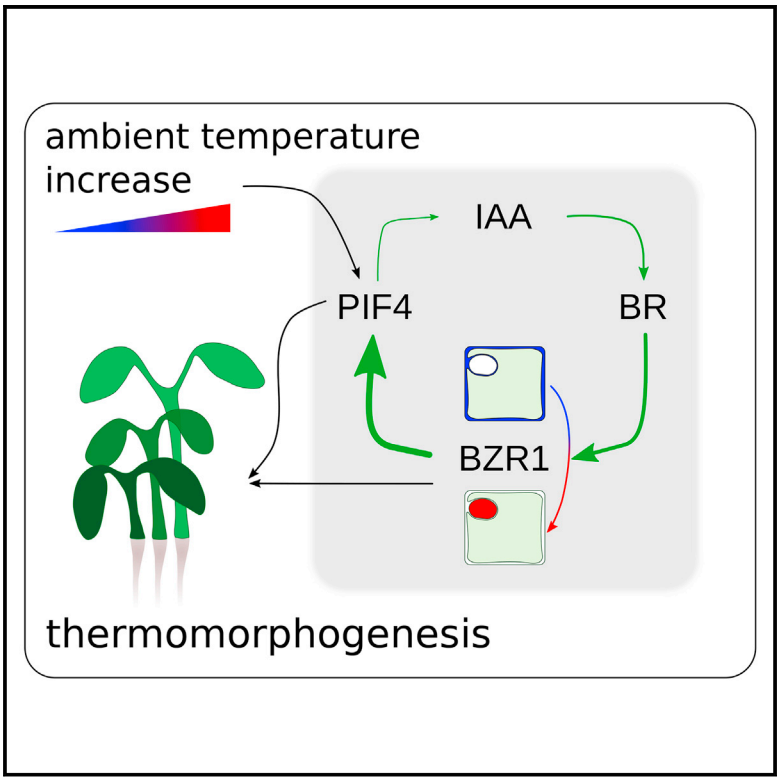


## Authors

Carla Ibañez, Carolin Delker, Cristina Martinez, ..., Korbinian Schneeberger, Salome Prat, Marcel Quint

## Correspondence

marcel.quint@landw.uni-halle.de

## In Brief

Ibañez et al. show that PIF4- and auxin-mediated growth responses in high temperature depend on brassinosteroids. In warmth, the transcription factor BZR1 accumulates in the nucleus and activates growth-response genes, likely in cooperation with PIF4. In addition, BZR1 provides an amplifying feedback loop by directly inducing *PIF4* transcription.

## Highlights

- Brassinosteroid biosynthesis and signaling mutants display thermomorphogenic defects
- PIF4- and auxin-mediated thermomorphogenesis is brassinosteroid dependent
- BZR1 accumulates in the nucleus at high temperature
- In warmth, BZR1 binds to the promoter of *PIF4* to increase its transcript levels

Ibañez et al., 2018, Current Biology *28*, 303–310
January 22, 2018 
https://doi.org/10.1016/j.cub.2017.11.077

CellPress

Current Biology
Report

# Brassinosteroids Dominate Hormonal Regulation of Plant Thermomorphogenesis via BZR1

Carla Ibañez,[1,2] Carolin Delker,[1,2] Cristina Martinez,[3] Katharina Bürstenbinder,[2] Philipp Janitza,[1,2] Rebecca Lippmann,[1] Wenke Ludwig,[1] Hequan Sun,[4] Geo Velikkakam James,[4] Maria Klecker,[5,6] Alexandra Grossjohann,[1,2] Korbinian Schneeberger,[4] Salome Prat,[3] and Marcel Quint[1,2,7,*]

[1]Institute of Agricultural and Nutritional Sciences, Martin Luther University Halle-Wittenberg, Betty-Heimann Strasse 5, 06120 Halle (Saale), Germany
[2]Department of Molecular Signal Processing, Leibniz Institute of Plant Biochemistry, Weinberg 3, 06120 Halle (Saale), Germany
[3]Department of Plant Molecular Genetics, Centro Nacional de Biotecnología-CSIC, Campus de Cantoblanco, Darwin 3, 28049 Madrid, Spain
[4]Department of Plant Developmental Biology, Max Planck Institute for Plant Breeding Research, 50829 Cologne, Germany
[5]Independent Junior Research Group on Protein Recognition and Degradation, Leibniz Institute of Plant Biochemistry, Weinberg 3, 06120 Halle (Saale), Germany
[6]ScienceCampus Halle – Plant-Based Bioeconomy, Betty-Heimann-Strasse 3, 06120 Halle (Saale), Germany
[7]Lead Contact
*Correspondence: marcel.quint@landw.uni-halle.de
https://doi.org/10.1016/j.cub.2017.11.077

## SUMMARY

Thermomorphogenesis is defined as the suite of morphological changes that together are likely to contribute to adaptive growth acclimation to usually elevated ambient temperature [1, 2]. While many details of warmth-induced signal transduction are still elusive, parallels to light signaling recently became obvious (reviewed in [3]). It involves photoreceptors that can also sense changes in ambient temperature [3–5] and act, for example, by repressing protein activity of the central integrator of temperature information PHYTOCHROME-INTERACTING FACTOR 4 (PIF4 [6]). In addition, *PIF4* transcript accumulation is tightly controlled by the evening complex member EARLY FLOWERING 3 [7, 8]. According to the current understanding, PIF4 activates growth-promoting genes directly but also via inducing auxin biosynthesis and signaling, resulting in cell elongation. Based on a mutagenesis screen in the model plant *Arabidopsis thaliana* for mutants with defects in temperature-induced hypocotyl elongation, we show here that both PIF4 and auxin function depend on brassinosteroids. Genetic and pharmacological analyses place brassinosteroids downstream of PIF4 and auxin. We found that brassinosteroids act via the transcription factor BRASSINAZOLE RESISTANT 1 (BZR1), which accumulates in the nucleus at high temperature, where it induces expression of growth-promoting genes. Furthermore, we show that at elevated temperature BZR1 binds to the promoter of *PIF4*, inducing its expression. These findings suggest that BZR1 functions in an amplifying feedforward loop involved in *PIF4* activation. Although numerous negative regulators of PIF4 have been described, we identify BZR1 here as a true temperature-dependent positive regulator of *PIF4*, acting as a major growth coordinator.

## RESULTS AND DISCUSSION

To contribute to a better understanding of the signaling pathways activated in plant shoots in response to elevated temperature, we previously used the thermo-hypersensitive accession Rrs-7 of the model plant *Arabidopsis thaliana* as a genetic background for a an EMS forward genetic screen [9, 10]. From this screen, we identified the *okapi1* (*opi1*) mutant, which was unable to elongate hypocotyls in response to warmth and encoded a novel allele in *DE-ETIOLATED 1* (*DET1* [9]). We found that DET1 modulates thermomorphogenesis via the CONSTITUTIVE PHOTOMORPHOGENIC 1/SUPPRESSOR OF PHYA-105 1 (COP1/SPA) complex and ultimately ELONGATED HYPOCOTYL 5 (HY5), which negatively regulates the central signaling hub PHYTOCHROME-INTERACTING FACTOR 4 (PIF4).

### The *opi3* and *opi7* Thermomorphogenic Mutants Correspond to Mutations in Brassinosteroid Biosynthetic Genes

Like *opi1*, *opi3* and *opi7* mutants displayed a defect in temperature-induced hypocotyl elongation (TIHE, Figure 1A). While cell number was slightly reduced only in *opi3* (Figure S1A), hypocotyl cells of both mutants were shorter at 28°C but not at 20°C, when compared to wild-type (Figure 1B). This suggests that *opi3* and *7* display primarily defects in warmth-specific cell elongation, besides being partly impaired in cell division. In addition to TIHE defects, both mutants also showed thermomorphogenic phenotypes in later vegetative development (Figures 1C, S1B, and S1C). Mapping by sequencing [11–14] of pools of the backcrossed mutant lines identified a non-synonymous mutation in the *AT3G02580* gene of *opi3*, causing a methionine to isoleucine change (Figure S1D). *AT3G02580* encodes *DWARF7 (DWF7) / STEROL 1 (STE1) / BOULE 1 (BUL1)*, which catalyzes the delta7 sterol C-5 desaturation step in brassinosteroid (BR) biosynthesis [15–17]. The same mapping by sequencing approach identified a

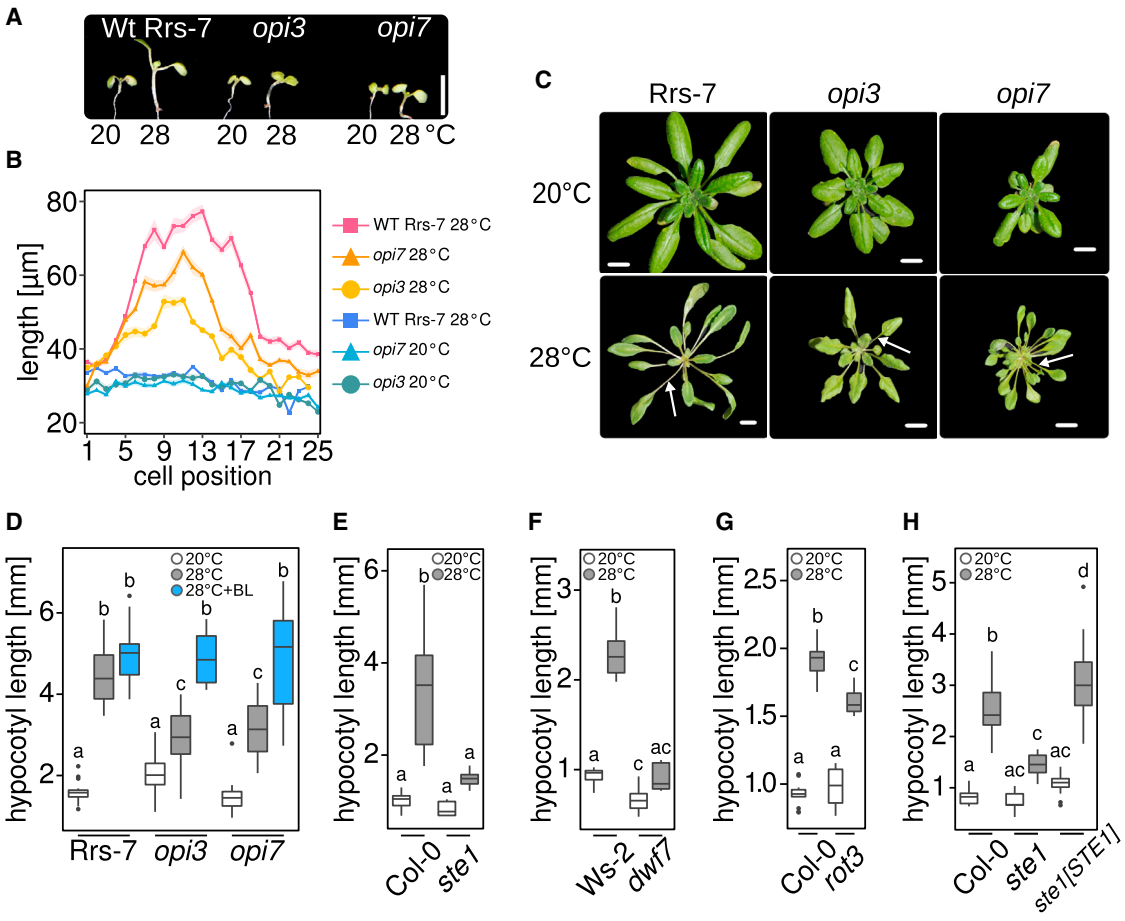


**Figure 1. *opi3* and *opi7* Identify a Central Role of Brassinosteroids in Thermomorphogenesis**

(A) Representative pictures of seedlings grown under LD photoperiods for either 7 days at constant 20°C or shifted on day 4 from 20°C to 28°C.

(B) Length of cortical hypocotyl cells according to their position along a longitudinal axis (pos. 1 = first cell from the shoot apex; pos. 25 = 25th cell from the shoot apex close to the hypocotyl-root junction). Lines show mean values ± SEM.

(C) Rosette phenotypes of 14-day-old plants grown constantly at either 20°C or 28°C. The arrows point to differences in petiole elongation at 28°C. (Quantifications are shown in Figure S1C.)

(D) Quantification of the assay displayed in (A) including rescue of the wild-type elongation response at 28°C in *opi3* and *opi7* by supplementing the media with 100 nM epi-BL.

(E and F) The *ste1-1* (Col-0 background) (E) and *dwf7-1* (Ws-2) (F) mutants phenocopy *opi3* in a TIHE assay.

(G) The *rot3-1* mutant (Col-0) phenocopies *opi7* in a TIHE assay.

(H) A *35S::STE1-YFP* construct in the *ste1-1* background transgenically complements the TIHE defect of the *ste1-1* mutant.

In (B) and (D)–(H), seedlings have been cultivated as described in (A). Horizontal bars, boxes, and whiskers show medians, interquartile ranges (IQR), and data ranges, respectively. Black dots mark outliers (defined as >1.5 × IQR). Different letters denote statistically significant differences as assessed by 1-way ANOVA followed by a Tukey HSD test ($p < 0.05$). See also Figure S1.

non-synonymous mutation in *AT4G36380* for *opi7*, causing a proline to leucine substitution (Figure S1D). *AT4G36380* encodes *ROTUNDIFOLIA 3* (*ROT3*/*CYP90C*), a cytochrome P-450 enzyme also involved in BR biosynthesis, most likely in the conversion step of typhasterol to castasterone [18, 19].

Identification of these two candidate genes supports an important role of BR biosynthesis in thermomorphogenesis, as already suggested by an earlier study reporting TIHE defects in the *det2* BR biosynthesis mutant [20]. In agreement with this, we were able to completely rescue the *opi3* and *opi7* TIHE defects at 28°C by exogenous application of the bioactive BR epi-brassinolide (BL, Figure 1D). Furthermore, phenocopies of both mutants in other genetic backgrounds (*opi3* – *dwf7-1* in Ws-2, *ste1-1* in Col-0; *opi7* – *rot3-1* in Col-0; Figures 1E–1G) confirm that defective function of these genes cause the *opi3* and *opi7* mutant phenotypes. These data, together with the transgenic complementation of the *ste1-1* mutant, which is allelic to *opi3* (Figure 1H), strongly support causality of the two candidate genes.

## BRs Directly Affect PIF4-Dependent Thermomorphogenesis Signaling

So far, our data are consistent with Gray et al. [20] and Stavang et al. [21] who had previously shown the general need for an intact BR pathway for thermomorphogenic shoot responses. We next asked whether BRs affect thermomorphogenesis via

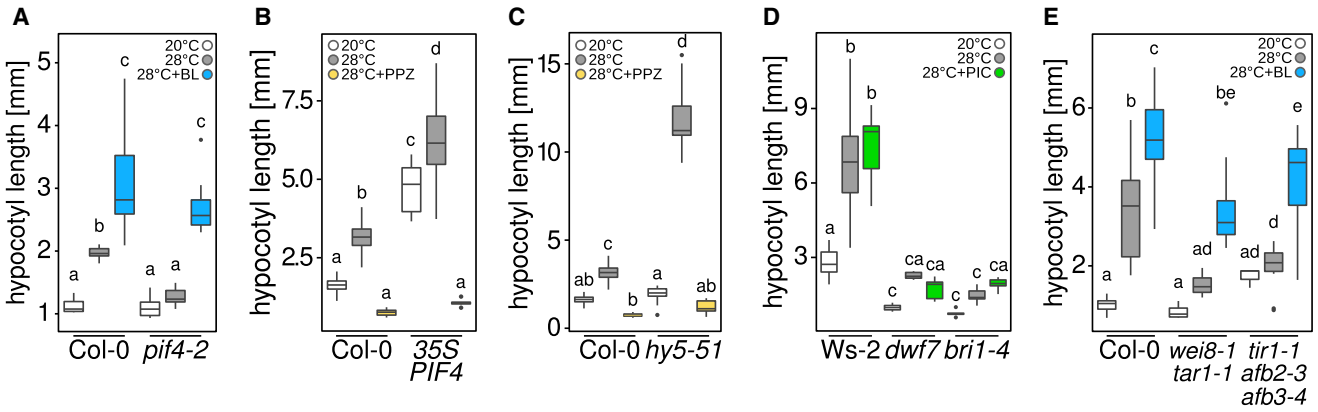


**Figure 2. Pharmacological and Genetic Analyses Place BRs Downstream of PIF4 and Auxin in Thermomorphogenesis Signaling**

(A) Exogenously applied BL (100 nM epi-BL) completely rescues the *pif4-2* TIHE defect.

(B and C) Application of the BR biosynthesis inhibitor propiconazole (PPZ, 1 μM) completely suppresses the hyperelongated hypocotyl phenotypes of (B) *35S::PIF4* and (C) *hy5-51* at 28°C.

(D) BR biosynthesis (*dwf7-1*) and signaling (*bri1-4*) mutants display TIHE defects that cannot be rescued by application of the synthetic auxin picloram (PIC, 5 μM).

(E) Auxin biosynthesis (*wei8-1 tar1-1*) and signaling (*tir1-1 afb2-3 afb3-4*) mutants display TIHE defects that can be rescued by exogenous application of BL (100 nM epi-BL).

In (A)–(E), TIHE assays have been performed under LD conditions as described in Figure 1. Horizontal bars, boxes, and whiskers show medians, interquartile ranges (IQR), and data ranges, respectively. Black dots mark outliers (defined as > 1.5 × IQR). Different letters denote statistically significant differences as assessed by 1-way ANOVA followed by a Tukey HSD test ($p < 0.05$). See also Figure S2.

the canonical PIF4-dependent signaling pathway and attempted to rescue the *pif4-2* loss-of-function mutant by supplementing 28°C grown seedlings with BL. As shown in Figure 2A, BL was able to rescue the *pif4-2* TIHE defect up to wild-type levels. Furthermore, blocking BR biosynthesis by exogenous application of the BR biosynthesis inhibitor propiconazole (PPZ) completely reverted the hyperelongating phenotype of *35S::PIF4* (Figure 2B) as well as loss-of-function alleles of the PIF4 repressors HY5 (*hy5-51*, Figure 2C) and EARLY FLOWERING 3 (*elf3-4*) (Figure S2A). Crossing the *dwf7-1* BR biosynthetic mutant, which is allelic to *opi3*, into the hyperelongating *elf3-4* background likewise reduced TIHE (Figure S2B), hence providing complementary genetic support for the pharmacological data. Altogether, both pharmacological and genetic studies suggest that BRs are part of the canonical thermomorphogenic pathway and regulate growth downstream of PIF4.

## BRs Act Downstream of Auxin and GA

PIF4 directly targets the promoters of auxin biosynthetic genes and thereby induces an increase in biologically active free auxin levels in a temperature-dependent manner [22, 23]. Consequently, growth-promoting auxin response genes like *SMALL AUXIN-UP RNAs* (*SAURs*) are induced via TRANSPORT INHIBITOR RESPONSE 1 / AUXIN SIGNALING F BOX (TIR1/AFBs) E3 ubiquitin ligase-mediated degradation of the negative Aux/IAA regulators, likely resulting in cell elongation. Furthermore, PIF4 has been shown to directly induce transcription of *SAURs* [22]. Extensive crosstalk between auxin and BR pathways has been described in multiple biological processes (for example, [24–26]), with signaling hierarchies of these two hormones changing from an upstream to downstream regulation, concerted or even antagonistic action, depending on the tissue and developmental context [24, 27–30].

We therefore aimed to dissect this hierarchy in a temperature-specific context, by using again a combination of pharmacological and genetic experiments. Specifically, we asked whether addition of BL was able to rescue the 28°C hypocotyl elongation defects of auxin biosynthesis and signaling mutants, and vice versa whether exogenous application of the synthetic auxin picloram (PIC), which is especially active in hypocotyls, was able to rescue the elongation defects of BR biosynthesis and signaling mutants at 28°C. Figure 2D shows that TIHE defects of both BR biosynthesis and signaling mutants could not be rescued by exogenous application of PIC. In contrast, exogenous application of BL rescued TIHE defects in auxin biosynthesis and signaling mutants (Figure 2E). However, as BL-treated auxin mutants were slightly shorter at 28°C than BL-treated WT, a residual BR-independent auxin activity cannot be excluded. But taken together, these observations suggest that BRs act downstream of auxin in thermomorphogenesis signaling.

In addition to auxin and BR, gibberellic acid (GA) also plays an important role in thermomorphogenesis, as stabilization of the DELLA repressors leads to sequestration of the PIF4 protein [31]. However, we observed that BL application can rescue the TIHE defect of the dominant-negative *gai-1D DELLA* mutant, and that PPZ treatment abolishes the constitutive temperature response of *della* pentuple mutants (Figure S2C). Based on these data, we propose that auxin and GA function in thermomorphogenesis is strictly dependent on BRs.

## BRs Regulate Thermomorphogenesis by Warmth-Induced Translocation of BZR1 to the Nucleus

As BR activity is primarily executed via the regulation of gene expression [32–34], we closely investigated the role of the BR-regulated transcription factor BRASSINAZOLE-RESISTANT 1 (BZR1 [32],) in the TIHE response. In line with a promoting role

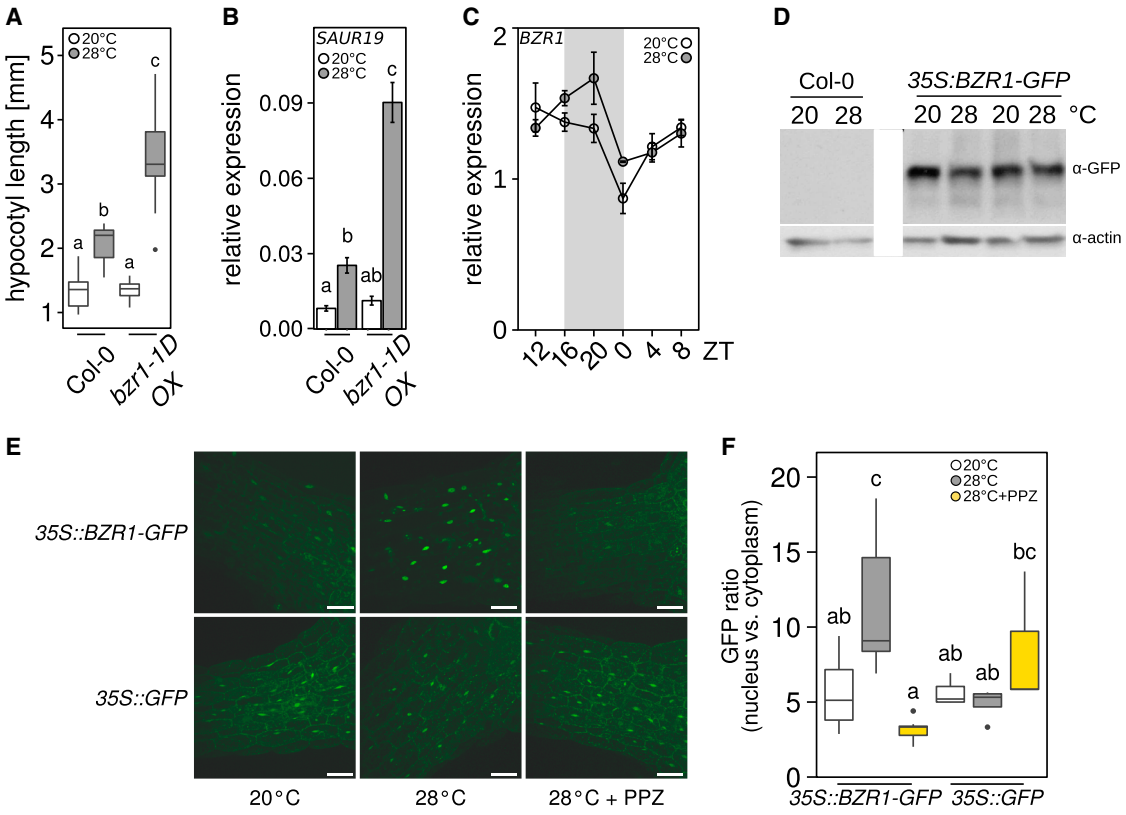


**Figure 3. BZR1 Positively Regulates TIHE by Warmth-Induced Accumulation in the Nucleus**

(A) The constitutively active *bzr1-1D-OX* allele hyperelongates specifically at 28°C in TIHE assays (performed as in Figure 1). Horizontal bars, boxes, and whiskers show medians, interquartile ranges (IQR), and data ranges, respectively. Black dots mark outliers (defined as > 1.5 × IQR).

(B) qRT-PCR analysis of *SAUR19* expression levels. Seedlings have been grown for 7 days at 20°C. Control plants were left at 20°C, and warmth-induced plants were shifted to 28°C at lights off (ZT16) and harvested at ZT20. *AT1G13320* (*PP2AA3*) served as the reference gene. Error bars represent SEM; n = 3 biological replicates.

(C) qRT-PCR experiment showing diurnal expression patterns of *BZR1* in plants grown for 7 days constantly at either 20°C or 28°C. No statistically significant differences were detected throughout all time points. Error bars represent SEM, n = 3 biological replicates.

(D) Western blot showing BZR1-GFP protein from 35S::BZR1-GFP and control Col-0 whole seedlings grown for 7 days constantly at 20°C or shifted on day 7 to 28°C at ZT10 and sampled at ZT23. BZR1 was detected with anti-GFP antibody.

(E) BZR1-GFP accumulates in the nucleus of elongating hypocotyl cells at high ambient temperatures, while the control 35S::GFP does not. Seedlings were treated as in (D). Confocal laser scanning microscopy images from the apical part of hypocotyls from representative seedlings are shown. Scale bars, 50 μm.

(F) Boxplot showing quantifications of images as shown in (E). GFP signal intensity ratios from nuclear versus cytoplasmic signals were measured. Horizontal bars, boxes, and whiskers show medians, interquartile ranges (IQR), and data ranges, respectively. Black dots mark outliers (defined as > 1.5 × IQR). n = 8 biological replicates.

In (A)–(C) and (F), different letters denote statistically significant differences as assessed by 1-way ANOVA followed by a Tukey HSD test ($p < 0.05$). (A-F) Seedlings have been grown under LD photoperiods. See also Figure S3.

of BRs in thermomorphogenesis, the gain-of-function *bzr1-1*D overexpressor (*bzr1-1D-OX* [35]) as well as an independent *35S::BZR1-GFP* line displayed a hypersensitive response to elevated temperature (Figures 3A and S3A). Interestingly, the hyperelongation response was strictly conditional and specific for 28°C, suggesting a higher activity of this transcription factor under warm temperatures. If so, BZR1 transcriptional activity should be detectable by warmth-induced upregulation of genes known to promote cell elongation such as members of the *SAUR* family. As shown in Figure 3B, *SAUR19* gene expression profiles mirror the hypersensitive hypocotyl phenotype at 28°C, whereas no difference between *bzr1-1D-OX* and wild-type plants could be observed at 20°C. The *35S::BZR1-GFP* allele largely behaves like *bzr1-1D-OX*, albeit *SAUR19* is already overexpressed at 20°C (Figure S3B). Together, this line of evidence suggests that, in a temperature context, BR action is executed via the BZR1 transcription factor. BZR1 is thus a positive regulator of thermomorphogenesis, promoting growth in a temperature-dependent manner.

According to the current understanding of BR signaling, in a low BR cellular environment, BZR1 is phosphorylated by the BRASSINOSTEROID-INSENSITIVE 2 (BIN2) shaggy-like kinase [36, 37], that inhibits its nuclear localization and DNA-binding activity [34]. Upon increasing BR levels, BIN2 is inactivated, resulting in BZR1 dephosphorylation, its accumulation in the nucleus and binding to conserved E- and G-boxes in the promoters of BR-responsive target genes [38]. Several scenarios for a molecular mechanism of BZR1 action in thermomorphogenesis are

therefore conceivable. Although the most simple scenario would be that temperature modulates BZR1 transcript and/or protein levels, we did not detect significant differences between 20°C and 28°C grown seedlings with regard to *BZR1* transcript accumulation (Figure 3C). Confirming previous reports [21, 33], we also did not observe changes in BZR1 protein levels at different temperatures (Figure 3D). Therefore, BZR1-induced transcriptional responses at elevated temperature do not seem to be linked to increased levels of this transcriptional regulator. We did, however, observe a change in BZR1 localization. When seedlings were shifted to 28°C, the nuclear-to-cytoplasmic ratio of BZR1-GFP protein was significantly increased as compared to seedlings kept at 20°C (Figures 3E and 3F for cells from the apical part of hypocotyls; Figures S3C and S3D for cells from the mid part of hypocotyls). PPZ treatment completely blocked this relocalization, indicating that this effect depends on functional BR biosynthesis (Figures 3E, 3F, and S3C, and S3D). In support of this scenario, BR biosynthesis genes have been reported to be upregulated at elevated temperature [21]. Furthermore, BR biosynthesis genes have been shown to be bound by PIF4 in both genome-wide chromatin immunoprecipitation sequencing (ChIP-seq) [33] as well as targeted ChIP-PCR experiments [39]. In confirmation of these observations, several of these genes seem to be downregulated in a *pif4* loss-of-function background ([40], Figure S3E). Collectively, this evidence suggests that warmth-induced BR biosynthesis may be PIF4 dependent. As a consequence, at elevated temperatures BZR1 is preferentially translocated to the nucleus, thereby contributing to temperature-induced growth. Although the failing relocalization in presence of PPZ would be consistent with changes in BZR1 phosphorylation patterns, this aspect remained inconclusive from our own experiments. Previous studies, however, reported that temperature has no effect on BZR1 phosphorylation patterns [33]. In summary, in contrast to roots, where BRs have a less pronounced effect in warmth and BZR1 seems to negatively regulate growth [41], our data support a scenario whereby BRs play a central role in shoot thermomorphogenesis by mediating warmth-induced translocation of BZR1 to the nucleus, where it induces transcription of genes with a role in promoting cell elongation.

Interestingly, several genes involved in cell elongation including *SAUR*s are common targets of BZR1, AUXIN RESPONSE FACTORs, and PIF4 [33, 34]. Oh et al. [33] showed that PIF4 and BZR1 cooperatively regulate hundreds of target genes by binding as a complex to their co-regulated targets. Importantly, BZR1 and PIF4 heterodimerization seems to be required for BZR1's growth-promoting activity and, conversely, BZR1 is required for PIF-mediated cell elongation [31, 33]. Based on these reports, it may be possible that increased amounts of BZR1 in the nucleus at elevated temperatures (Figures 3E, 3F, S3C, and S3D) need similarly increased amounts of PIF4 to efficiently induce transcription of growth-promoting genes. Given that both PIF4 mRNA and protein levels do indeed increase in warmth (e.g., [6, 33, 42]), this seems to be a reasonable scenario.

## BRs Positively Regulate *PIF4* Expression via the Transcription Factor BZR1

While various negative transcriptional and post-transcriptional regulators of PIF4 with a demonstrated or predicted role in a temperature context have been described [e.g., 7–9, 21, 42–44], positive regulators involved in increased *PIF4* transcription at elevated temperatures are largely unknown. It is therefore poorly understood how elevated temperatures trigger *PIF4* mRNA accumulation and subsequently lead to increased protein levels. We speculated whether BZR1 itself may act as a temperature-dependent positive regulator of *PIF4* transcription, in addition to its co-activation role with PIF4. If so, it could act in a direct feedforward loop on *PIF4* expression, to accelerate or amplify temperature responses.

Indeed, while no difference was observed in *PIF4* expression levels between wild-type and *bzr1-1D-OX* and *35S::BZR1-GFP* at 20°C, a strong and moderate overexpression of the *PIF4* transcript was observed in *bzr1-1d-OX* and *35S::BZR1-GFP* at 28°C, respectively (Figure 4A). This suggests that BZR1 is involved in *PIF4* activation specifically at elevated ambient temperatures. To assess whether BZR1 may directly control *PIF4* expression, we performed transient transactivation protoplast assays. Here, co-transfection of the *PIF4pro:LUC* reporter and *CFP* control constructs into *Arabidopsis* protoplasts resulted in poor expression of the *PIF4pro:LUC* construct (Figure 4B). However, when the reporter was co-transfected with *35S::BZR1-GFP*, we observed high levels of LUC activity (Figure 4B), indicating that BZR1 is able to regulate *PIF4* expression by binding to its promoter.

A closer inspection of the *PIF4* promoter sequence identified E-box and G-box elements (Figure 4C), both of which were shown to be enriched in the promoters of genes that are upregulated by BZR1 [33]. To test whether BZR1 directly binds to these motifs *in vivo* and to assess whether this interaction is temperature sensitive, we performed ChIP-qPCR assays. To this end, BZR1 was immunoprecipitated out of *35S::BZR1-GFP* plants by using an anti-GFP antibody. Binding to the *PIF4* promoter was assayed with primers specific to the E- and G-box elements. Figure 4D shows that binding of BZR1 to both E-/G-boxes hardly exceeds the background control PP2AA3 in plants grown at 20°C. When plants were shifted to 28°C, however, BZR1 occupancy of the *PIF4* promoter E-/G-boxes was notably increased, coinciding with *PIF4* transcript upregulation in response to warmth. As such, BZR1-mediated upregulation of *PIF4* transcript levels identifies a positive amplification loop, potentially involved in extended warmth-induced elongation growth.

## Synthesis and Conclusions

This study establishes a role of BRs in the canonical PIF4-dependent signaling pathway regulating thermomorphogenic responses in *A. thaliana* above ground tissues. Based on genetics and pharmacological studies, we identified an important function of BRs downstream of auxin and PIF4. Dependency of PIF4 and auxin action on BR synthesis indicates that BR signaling, which triggers temperature-sensitive nuclear localization of the transcription factor BZR1, plays a dominant role in this triumvirate. However, given that all components in this seemingly linear signaling cascade activate a common set of target genes in a temperature-sensitive manner, the final output appears to be more complex (Figure 4E). While we did not directly address the specific function of auxin in this response, we found that BRs positively regulate *PIF4* transcription in warmth, via BZR1. This suggests that this feedforward regulation promotes *PIF4*

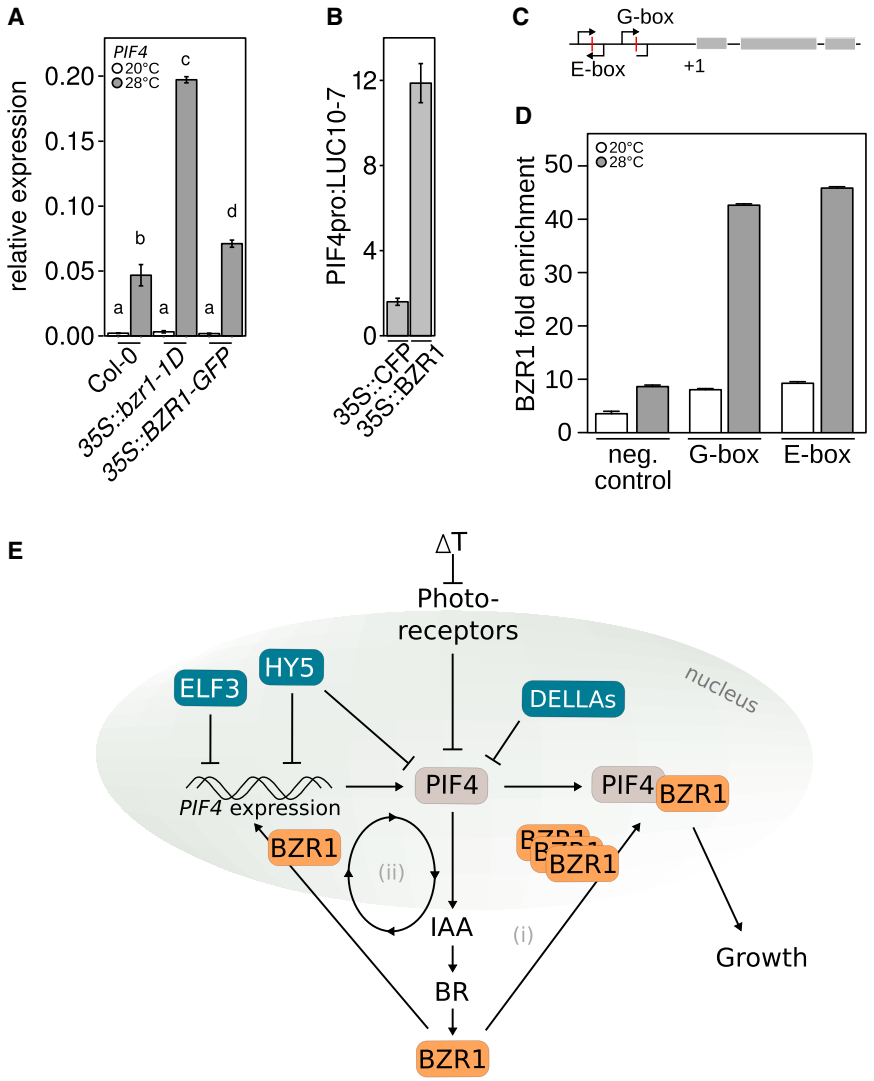


**Figure 4. BZR1 Positively Regulates *PIF4* Expression at Elevated Temperatures**

(A) qRT-PCR analysis of *PIF4* expression levels. Seedlings have been grown for 7 days at 20°C. Control plants were left at 20°C, and warmth-induced plants were shifted to 28°C at lights off (ZT16) and harvested 4 hr later at ZT20. *AT1G13320* (*PP2AA3*) served as the reference gene. Error bars represent SEM, n = 3 biological replicates. In (A)–(D), seedlings were grown under LD photoperiods and were treated as in Figure 3D.

(B) Protoplast assays of Col-0 mesophyll cells in which a PIF4pro:LUC was co-transfected with either a *CFP* (negative control) or *BZR1* construct.

(C) Simplified *PIF4* gene structure with G- and E-boxes in the promoter.

(D) BZR1 directly binds to the promoter of *PIF4*. ChIP of BZR1 using *35S::BZR1-GFP* seedlings (either grown at constant 20°C or shifted to 28°C) show enrichment at G- and E-boxes in the *PIF4* promoter in 28°C seedlings. *AT1G13320* (*PP2AA3*) was used as a negative control. Error bars show SEM of technical replicates. Seedlings were treated as described in Figure 3D. The experiment has been independently repeated with similar results.

(E) Simplified model integrating the mechanism identified in this study into the current understanding of PIF4-dependent shoot thermomorphogenesis signaling. In this model, BRs act downstream of PIF4 and auxin to regulate elongation growth via BZR1 in response to elevated ambient temperatures. In a response amplifying feed forward loop, BZR1 may induce *PIF4* transcription, possibly in complex with other PIFs (not shown here), to (1) enable efficient cooperative activation of growth-promoting genes, and (2) to enhance the PIF4 > auxin > BR part of the pathway.

transcription (possibly in complex with other PIFs) and leads to accumulation of both transcription factors, which is required for efficient co-activation of growth-promoting genes [31, 33]. Independent of this co-operative manner of gene regulation, warmth-induced upregulation of *PIF4* transcript via BZR1 generates a general amplifying loop that increases the PIF4 > auxin > BR cascade of the thermomorphogenesis signaling pathway. In any case, in a sea of negative regulators of PIF4 function (reviewed in [2, 43]), BRs/BZR1 might represent the only so far known true positive regulator(s) of *PIF4* in a temperature context. The otherwise tight negative regulation of PIF4 mRNA and protein levels by a multitude of other factors (reviewed in [2]) may therefore be necessary to control "infinite" elongation growth via the mechanism proposed in this study.

## STAR★METHODS

Detailed methods are provided in the online version of this paper and include the following:

- KEY RESOURCES TABLE
- CONTACT FOR REAGENT AND RESOURCE SHARING
- EXPERIMENTAL MODEL AND SUBJECT DETAILS
- METHOD DETAILS
  - EMS screen
  - TIHE assays and growth conditions
  - Hypocotyl cell measurements
  - Rosette and petiole measurements
  - Confocal laser scanning microscopy and image analysis for subcellular localization
  - RNA extraction, cDNA synthesis, and qRT-PCR
  - Protoplast transient expression assay
  - ChIP-PCR
  - Protein extraction and western blot
- QUANTIFICATION AND STATISTICAL ANALYSIS

## SUPPLEMENTAL INFORMATION

Supplemental Information includes three figures and can be found with this article online at https://doi.org/10.1016/j.cub.2017.11.077.

## ACKNOWLEDGMENTS

We thank Luz Irina A. Calderon Villalobos, Sunghwa Choe, Daniele Silvestro, and Zhiyong Wang for sharing seeds and Lennart Eschen-Lippold, Daphne Ezer, Frederik Faden, Giulia Furlan, Martin Weyhe, and Philip Wigge for technical support and sharing data and/or materials. The authors furthermore thank Miroslav Strnad and Dana Tarkuwska. We acknowledge Bill Gray for comments on the manuscript and Michael Lenhard for conceptual input. This study was supported by a Spanish MINECO grant (BIO2014-60064-R) to S.P. and a grant from the Deutsche Forschungsgemeinschaft to M.Q. (Qu 141/3-1). Collaboration between the Prat and Quint labs was enabled by a short-term EMBO fellowship to C.I. (ASTF 593-2016).

## AUTHOR CONTRIBUTIONS

C.I., C.D., S.P., and M.Q. conceived and designed the experiments. C.I., C.D., C.M., M.K., A.G., R.L., W.L., K.B., and M.Q. performed the experiments. C.I., C.D., C.M., H.S., G.V.J., P.J., K.B., and K.S. analyzed the data. P.J. contributed reagents, materials, analysis, and tools. C.I. and M.Q. wrote the paper.

## DECLARATION OF INTERESTS

The authors declare no competing interests.

Received: September 5, 2017
Revised: November 9, 2017
Accepted: November 30, 2017
Published: January 11, 2018

## REFERENCES

1. Erwin, J.E., Heins, R.D., and Karlsson, M.G. (1989). Thermomorphogenesis in *Lilium longiflorum*. Am. J. Bot. *76*, 47–52.
2. Quint, M., Delker, C., Franklin, K.A., Wigge, P.A., Halliday, K.J., and van Zanten, M. (2016). Molecular and genetic control of plant thermomorphogenesis. Nat. Plants *2*, 15190.
3. Legris, M., Klose, C., Burgie, E.S., Rojas, C.C., Neme, M., Hiltbrunner, A., Wigge, P.A., Schäfer, E., Vierstra, R.D., and Casal, J.J. (2016). Phytochrome B integrates light and temperature signals in *Arabidopsis*. Science *354*, 897–900.
4. Jung, J.-H., Domijan, M., Klose, C., Biswas, S., Ezer, D., Gao, M., Khattak, A.K., Box, M.S., Charoensawan, V., Cortijo, S., et al. (2016). Phytochromes function as thermosensors in *Arabidopsis*. Science *354*, 886–889.
5. Fujii, Y., Tanaka, H., Konno, N., Ogasawara, Y., Hamashima, N., Tamura, S., Hasegawa, S., Hayasaki, Y., Okajima, K., and Kodama, Y. (2017). Phototropin perceives temperature based on the lifetime of its photoactivated state. Proc. Natl. Acad. Sci. USA *114*, 9206–9211.
6. Koini, M.A., Alvey, L., Allen, T., Tilley, C.A., Harberd, N.P., Whitelam, G.C., and Franklin, K.A. (2009). High temperature-mediated adaptations in plant architecture require the bHLH transcription factor PIF4. Curr. Biol. *19*, 408–413.
7. Raschke, A., Ibañez, C., Ullrich, K.K., Anwer, M.U., Becker, S., Glöckner, A., Trenner, J., Denk, K., Saal, B., Sun, X., et al. (2015). Natural variants of ELF3 affect thermomorphogenesis by transcriptionally modulating PIF4-dependent auxin response genes. BMC Plant Biol. *15*, 197.
8. Box, M.S., Huang, B.E., Domijan, M., Jaeger, K.E., Khattak, A.K., Yoo, S.J., Sedivy, E.L., Jones, D.M., Hearn, T.J., Webb, A.A.R., et al. (2015). ELF3 controls thermoresponsive growth in *Arabidopsis*. Curr. Biol. *25*, 194–199.
9. Delker, C., Sonntag, L., James, G.V., Janitza, P., Ibañez, C., Ziermann, H., Peterson, T., Denk, K., Mull, S., Ziegler, J., et al. (2014). The DET1-COP1-HY5 pathway constitutes a multipurpose signaling module regulating plant photomorphogenesis and thermomorphogenesis. Cell Rep. *9*, 1983–1989.
10. Ibañez, C., Poeschl, Y., Peterson, T., Bellstädt, J., Denk, K., Gogol-Döring, A., Quint, M., and Delker, C. (2017). Ambient temperature and genotype differentially affect developmental and phenotypic plasticity in *Arabidopsis thaliana*. BMC Plant Biol. *17*, 114.
11. James, G.V., Patel, V., Nordström, K.J., Klasen, J.R., Salomé, P.A., Weigel, D., and Schneeberger, K. (2013). User guide for mapping-by-sequencing in *Arabidopsis*. Genome Biol. *14*, R61.
12. Schlötterer, C., Tobler, R., Kofler, R., and Nolte, V. (2014). Sequencing pools of individuals - mining genome-wide polymorphism data without big funding. Nat. Rev. Genet. *15*, 749–763.
13. Schneeberger, K. (2014). Using next-generation sequencing to isolate mutant genes from forward genetic screens. Nat. Rev. Genet. *15*, 662–676.
14. Schneeberger, K., Ossowski, S., Lanz, C., Juul, T., Petersen, A.H., Nielsen, K.L., Jørgensen, J.-E., Weigel, D., and Andersen, S.U. (2009). SHOREmap: Simultaneous mapping and mutation identification by deep sequencing. Nat. Methods *6*, 550–551.
15. Catterou, M., Dubois, F., Schaller, H., Aubanelle, L., Vilcot, B., Sangwan-Norreel, B.S., and Sangwan, R.S. (2001). Brassinosteroids, microtubules and cell elongation in *Arabidopsis thaliana*. I. Molecular, cellular and physiological characterization of the *Arabidopsis* bull mutant, defective in the delta 7-sterol-C5-desaturation step leading to brassinosteroid biosynthesis. Planta *212*, 659–672.
16. Choe, S., Noguchi, T., Fujioka, S., Takatsuto, S., Tissier, C.P., Gregory, B.D., Ross, A.S., Tanaka, A., Yoshida, S., Tax, F.E., and Feldmann, K.A. (1999). The *Arabidopsis dwf7/ste1* mutant is defective in the delta7 sterol C-5 desaturation step leading to brassinosteroid biosynthesis. Plant Cell *11*, 207–221.
17. Gachotte, D., Meens, R., and Benveniste, P. (1995). An *Arabidopsis* mutant deficient in sterol biosynthesis: heterologous complementation by ERG 3 encoding a delta 7-sterol-C-5-desaturase from yeast. Plant J. *8*, 407–416.
18. Kim, G.T., Tsukaya, H., and Uchimiya, H. (1998). The ROTUNDIFOLIA3 gene of *Arabidopsis thaliana* encodes a new member of the cytochrome P-450 family that is required for the regulated polar elongation of leaf cells. Genes Dev. *12*, 2381–2391.
19. Kim, G.-T., Fujioka, S., Kozuka, T., Tax, F.E., Takatsuto, S., Yoshida, S., and Tsukaya, H. (2005). CYP90C1 and CYP90D1 are involved in different steps in the brassinosteroid biosynthesis pathway in *Arabidopsis thaliana*. Plant J. *41*, 710–721.
20. Gray, W.M., Ostin, A., Sandberg, G., Romano, C.P., and Estelle, M. (1998). High temperature promotes auxin-mediated hypocotyl elongation in *Arabidopsis*. Proc. Natl. Acad. Sci. USA *95*, 7197–7202.
21. Stavang, J.A., Gallego-Bartolomé, J., Gómez, M.D., Yoshida, S., Asami, T., Olsen, J.E., García-Martínez, J.L., Alabadí, D., and Blázquez, M.A. (2009). Hormonal regulation of temperature-induced growth in *Arabidopsis*. Plant J. *60*, 589–601.
22. Franklin, K.A., Lee, S.H., Patel, D., Kumar, S.V., Spartz, A.K., Gu, C., Ye, S., Yu, P., Breen, G., Cohen, J.D., et al. (2011). Phytochrome-interacting factor 4 (PIF4) regulates auxin biosynthesis at high temperature. Proc. Natl. Acad. Sci. USA *108*, 20231–20235.
23. Sun, J., Qi, L., Li, Y., Chu, J., and Li, C. (2012). PIF4-mediated activation of YUCCA8 expression integrates temperature into the auxin pathway in regulating *Arabidopsis* hypocotyl growth. PLoS Genet. *8*, e1002594.
24. Halliday, K.J. (2004). Plant hormones: the interplay of brassinosteroids and auxin. Curr. Biol. *14*, R1008–R1010.
25. Hardtke, C.S. (2007). Transcriptional auxin-brassinosteroid crosstalk: who's talking? BioEssays *29*, 1115–1123.
26. Nemhauser, J.L., Mockler, T.C., and Chory, J. (2004). Interdependency of brassinosteroid and auxin signaling in *Arabidopsis*. PLoS Biol. *2*, E258.
27. Abbas, M., Alabadí, D., and Blázquez, M.A. (2013). Differential growth at the apical hook: all roads lead to auxin. Front. Plant Sci. *4*, 441.
28. Bao, F., Shen, J., Brady, S.R., Muday, G.K., Asami, T., and Yang, Z. (2004). Brassinosteroids interact with auxin to promote lateral root development in *Arabidopsis*. Plant Physiol. *134*, 1624–1631.

29. Chaiwanon, J., and Wang, Z.-Y. (2015). Spatiotemporal brassinosteroid signaling and antagonism with auxin pattern stem cell dynamics in *Arabidopsis* roots. Curr. Biol. *25*, 1031–1042.
30. Chung, Y., Maharjan, P.M., Lee, O., Fujioka, S., Jang, S., Kim, B., Takatsuto, S., Tsujimoto, M., Kim, H., Cho, S., et al. (2011). Auxin stimulates DWARF4 expression and brassinosteroid biosynthesis in *Arabidopsis*. Plant J. *66*, 564–578.
31. de Lucas, M., and Prat, S. (2014). PIFs get BRright: PHYTOCHROME INTERACTING FACTORs as integrators of light and hormonal signals. New Phytol. *202*, 1126–1141.
32. He, J.-X., Gendron, J.M., Sun, Y., Gampala, S.S., Gendron, N., Sun, C.Q., and Wang, Z.Y. (2005). BZR1 is a transcriptional repressor with dual roles in brassinosteroid homeostasis and growth responses. Science *307*, 1634–1638.
33. Oh, E., Zhu, J.-Y., and Wang, Z.-Y. (2012). Interaction between BZR1 and PIF4 integrates brassinosteroid and environmental responses. Nat. Cell Biol. *14*, 802–809.
34. Oh, E., Zhu, J.-Y., Bai, M.-Y., Arenhart, R.A., Sun, Y., and Wang, Z.-Y. (2014). Cell elongation is regulated through a central circuit of interacting transcription factors in the *Arabidopsis* hypocotyl. eLife *3*, e03031.
35. Oh, E., Zhu, J.-Y., Ryu, H., Hwang, I., and Wang, Z.-Y. (2014). TOPLESS mediates brassinosteroid-induced transcriptional repression through interaction with BZR1. Nat. Commun. *5*, 4140.
36. Wang, W., Bai, M.-Y., and Wang, Z.-Y. (2014). The brassinosteroid signaling network-a paradigm of signal integration. Curr. Opin. Plant Biol. *21*, 147–153.
37. Bernardo-García, S., de Lucas, M., Martínez, C., Espinosa-Ruiz, A., Davière, J.-M., and Prat, S. (2014). BR-dependent phosphorylation modulates PIF4 transcriptional activity and shapes diurnal hypocotyl growth. Genes Dev. *28*, 1681–1694.
38. Wang, Z.-Y., Bai, M.-Y., Oh, E., and Zhu, J.-Y. (2012). Brassinosteroid signaling network and regulation of photomorphogenesis. Annu. Rev. Genet. *46*, 701–724.
39. Wei, Z., Yuan, T., Tarkowská, D., Kim, J., Nam, H.G., Novák, O., He, K., Gou, X., and Li, J. (2017). Brassinosteroid biosynthesis is modulated via a transcription factor cascade of COG1, PIF4, and PIF5. Plant Physiol. *174*, 1260–1273.
40. Ezer, D., Shepherd, S.J.K., Brestovitsky, A., Dickinson, P., Cortijo, S., Charoensawan, V., Box, M.S., Biswas, S., Jaeger, K.E., and Wigge, P.A. (2017). The G-box transcriptional regulatory code in *Arabidopsis*. Plant Physiol. *175*, 628–640.
41. Martins, S., Montiel-Jorda, A., Cayrel, A., Huguet, S., Roux, C.P.-L., Ljung, K., and Vert, G. (2017). Brassinosteroid signaling-dependent root responses to prolonged elevated ambient temperature. Nat. Commun. *8*, 309.
42. Gangappa, S.N., and Kumar, S.V. (2017). DET1 and HY5 Control PIF4-mediated thermosensory elongation growth through distinct mechanisms. Cell Rep. *18*, 344–351.
43. Delker, C., van Zanten, M., and Quint, M. (2017). Thermosensing enlightened. Trends Plant Sci. *22*, 185–187.
44. Zhang, B., Holmlund, M., Lorrain, S., Norberg, M., Bakó, L., Fankhauser, C., and Nilsson, O. (2017). BLADE-ON-PETIOLE proteins act in an E3 ubiquitin ligase complex to regulate PHYTOCHROME INTERACTING FACTOR 4 abundance. eLife *6*, e26759.
45. Cheng, H., Qin, L., Lee, S., Fu, X., Richards, D.E., Cao, D., Luo, D., Harberd, N.P., and Peng, J. (2004). Gibberellin regulates *Arabidopsis* floral development via suppression of DELLA protein function. Development *131*, 1055–1064.
46. Peng, J., and Harberd, N.P. (1993). Derivative alleles of the *Arabidopsis* Gibberellin-insensitive (gai) mutation confer a wild-type phenotype. Plant Cell *5*, 351–360.
47. Silvestro, D., Andersen, T.G., Schaller, H., and Jensen, P.E. (2013). Plant sterol metabolism. Δ(7)-Sterol-C5-desaturase (STE1/DWARF7), Δ(5,7)-sterol-Δ(7)-reductase (DWARF5) and Δ(24)-sterol-Δ(24)-reductase (DIMINUTO/DWARF1) show multiple subcellular localizations in *Arabidopsis thaliana* (Heynh) L. PLoS ONE *8*, e56429.
48. Lorrain, S., Allen, T., Duek, P.D., Whitelam, G.C., and Fankhauser, C. (2008). Phytochrome-mediated inhibition of shade avoidance involves degradation of growth-promoting bHLH transcription factors. Plant J. *53*, 312–323.
49. Parry, G., Calderon-Villalobos, L.I., Prigge, M., Peret, B., Dharmasiri, S., Itoh, H., Lechner, E., Gray, W.M., Bennett, M., and Estelle, M. (2009). Complex regulation of the TIR1/AFB family of auxin receptors. Proc. Natl. Acad. Sci. USA *106*, 22540–22545.
50. Lincoln, C., Britton, J.H., and Estelle, M. (1990). Growth and development of the axr1 mutants of *Arabidopsis*. Plant Cell *2*, 1071–1080.
51. Czechowski, T., Stitt, M., Altmann, T., Udvardi, M.K., and Scheible, W.-R. (2005). Genome-wide identification and testing of superior reference genes for transcript normalization in *Arabidopsis*. Plant Physiol. *139*, 5–17.
52. Wu, F.-H., Shen, S.-C., Lee, L.-Y., Lee, S.-H., Chan, M.-T., and Lin, C.-S. (2009). Tape-*Arabidopsis* Sandwich - a simpler *Arabidopsis* protoplast isolation method. Plant Methods *5*, 16.
53. Yoo, S.-D., Cho, Y.-H., and Sheen, J. (2007). *Arabidopsis* mesophyll protoplasts: a versatile cell system for transient gene expression analysis. Nat. Protoc. *2*, 1565–1572.
54. Lee, J., He, K., Stolc, V., Lee, H., Figueroa, P., Gao, Y., Tongprasit, W., Zhao, H., Lee, I., and Deng, X.W. (2007). Analysis of transcription factor HY5 genomic binding sites revealed its hierarchical role in light regulation of development. Plant Cell *19*, 731–749.

## STAR★METHODS

### KEY RESOURCES TABLE

| REAGENT or RESOURCE | SOURCE | IDENTIFIER |
|---|---|---|
| Antibodies | | |
| Rabbit anti-GFP polyclonal antibody | MBL International | AB_591816 |
| Goat anti-rabbit IgG-HRP antibody | Santa Cruz Biotechnology | AB_631746 |
| Mouse anti-plant actin monoclonal antibody | Sigma-Aldrich | AB_476670 |
| Goat anti-mouse IgG (H+L) secondary antibody, HRP | Thermo Fisher Scientific | AB_228307 |
| Bacterial and Virus Strains | | |
| *E.coli* strain DH5α | N/A | N/A |
| Chemicals, Peptides, and Recombinant Proteins | | |
| Epi-Brassinolide | Sigma-Aldrich | Cat. E1641 |
| Propiconazole | Sigma-Aldrich | Cat. 45642 |
| Critical Commercial Assays | | |
| MinElute Reaction CleanUp kit | QIAGEN | 28204 |
| Experimental Models: Organisms/Strains | | |
| *Arabidopsis: Wt Col-0* | NASC | N1092 |
| *Arabidopsis: Wt Rrs7* | NASC | N22688 |
| *Arabidopsis: Wt Ws-2* | NASC | N2360 |
| *Arabidopsis: Wt Ler-1* | NASC | N22686 |
| *Arabidopsis: hy5-51* | NASC | N596651 |
| *Arabidopsis: elf3-4* | NASC | N3790 |
| *Arabidopsis: rot3-1* | NASC | N3727 |
| *Arabidopsis: bri1-4* | NASC | N3953 |
| *Arabidopsis: pif4-2* | NASC | N66043 |
| *Arabidopsis: della pentuple* | [45] | N/A |
| *Arabidopsis: gai1-D* | [46] | N/A |
| *Arabidopsis: wei8-4/tar1-1* | NASC | N16412 |
| *Arabidopsis: ste1* | [47] | N/A |
| *Arabidopsis: 35S::STE1-YFP* | [47] | N/A |
| *Arabidopsis: 35S::PIF4* | [48] | N/A |
| *Arabidopsis: bzr1-D Ox* | [35] | N/A |
| *Arabidopsis: dwf7-1* | [16] | N/A |
| *Arabidopsis: tir1-1 afb2-3 afb3-4* | [49] | N/A |
| *Arabidopsis: 35S::BZR1-GFP* | Salome Prat | N/A |
| *Arabidopsis: opi7* | This study | N/A |
| *Arabidopsis: opi3* | This study | N/A |
| Oligonucleotides | | |
| *PIF4_F* AGATGCAGCCGATGGAGATG | This study | N/A |
| *PIF4_R* GCTCACCAACCTAGTGGTCC | This study | N/A |
| *SAUR19_F* CTTCAAGAGCTTCATAATAATTCAAACTT | This study | N/A |
| *SAUR19_R* GAAGGAAAAAATGTTGGATCATCTT | This study | N/A |
| *SAUR15_F* AAGAGGATTCATGGCGGTCTATG | This study | N/A |
| *SAUR15_R* GTA TTG TTA AGC CGC CCA TTG G | This study | N/A |
| *BZR1_F* ACCTGGTGAGATAGCTGGGA | This study | N/A |
| *BZR1_R* GATGAGACCGGTGGGGTAAC | This study | N/A |
| *PIF4pro1 F* CTTCACTTGTATGTGTCCCACT | This study | N/A |

(*Continued on next page*)

| Continued | | |
|---|---|---|
| REAGENT or RESOURCE | SOURCE | IDENTIFIER |
| *PIF4pro1 R* CTCTAGGGACAACAGTACTG | This study | N/A |
| *PIF4pro2 F* CCGTATGGTCAAAATTATAT | This study | N/A |
| *PIF4pro2 R* TCCTGAAATGTATATCATTAA | This study | N/A |
| Recombinant DNA | | |
| *pNHL10::PIF4pro* | This study | N/A |
| *35S::BZR1* | This study | N/A |
| *35S::CFP* | Justin Lee (Leibniz Institute of Plant Biochemistry, Halle/Saale, Germany) | N/A |
| Software and Algorithms | | |
| RootDetection | N/A | http://www.labutils.de/rd.html |
| R | N/A | https://www.r-project.org/ |
| ImageJ | N/A | https://imagej.net/Welcome |

## CONTACT FOR REAGENT AND RESOURCE SHARING

Further information and requests for resources and reagents should be directed to and will be fulfilled by the Lead Contact, Marcel Quint (marcel.quint@landw.uni-halle.de).

## EXPERIMENTAL MODEL AND SUBJECT DETAILS

The *Arabidopsis thaliana* (L.) accessions Rrs-7, Col-0, Ws-2 and Ler-1, as well as mutants and transgenic lines were obtained from the Nottingham *Arabidopsis* Stock Centre (NASC) or from the references listed in the Key Resources Table.

## METHOD DETAILS

### EMS screen

Ethyl methanesulfonate (EMS)-mutagenized Rrs-7 seedlings were screened for alterations in the extent of hypocotyl elongation in response to a moderate temperature increase from 20°C to 28°C. Mutagenesis and mutant isolation was performed as described in Delker et al. [9].

### TIHE assays and growth conditions

Seeds were surface sterilized, stratified in sterile water at 4°C for 4 days, and placed in horizontal rows on vertically oriented plates containing *Arabidopsis thaliana* solution medium (ATS; [50]). Seedlings were cultivated for 3 days at 20°C before being separated into two groups. The control and warmth-induced group were cultivated for additional 4 days at 20°C or 28°C, respectively. At day 7, digital images of plates were taken and the different phenotypes were analyzed with RootDetection software (http://www.labutils.de/rd.html). Each assay contained at least 10 biological replicates. Plants were grown under a long day diurnal light cycle (16 hr light/8 hr dark) with 90 μmol $m^{-2}s^{-1}$ of photosynthetically active radiation (white light by T5 4000K fluorescence lamps). For hormone treatments, seeds were placed in horizontal rows on vertically oriented ATS plates containing the hormones/inhibitors at the concentrations specified for each assay. Epi-BL and PPZ stocks were diluted in ethanol (See Key Resources Table).

### Hypocotyl cell measurements

Cell number and size of hypocotyl cells were analyzed in 7-day-old seedlings ($n > 7$). Cell length of hypocotyl cortical cells was visualized by staining the cell wall with propidium iodide. Confocal pictures were taken and analyzed by ImageJ. Measurements were done from the top of the hypocotyl (petiole node – Cell number 1) to the bottom where the root-hypocotyl transition zone starts (collet area).

### Rosette and petiole measurements

Seeds were surface sterilized, and incubated in sterile water at 4°C for 4 days. After stratification, seeds were placed on soil and equally germinated at 20°C for 3 days. After 3 days at 20°C, one tray containing 20 replicates of each line was shifted to 28°C while a second tray was kept at 20°C as control. Light intensity at both temperatures was 250 μmol $m^{-2}s^{-1}$. Rosette pictures of 14 days-equally-developed plants ($n > 7$) were taken. Rosette area and petiole length was measured with ImageJ. Pots were randomized periodically.

### Confocal laser scanning microscopy and image analysis for subcellular localization

Images were taken with a Zeiss LSM 780 inverted microscope using a 40x water-immersion objective, and an excitation wavelength of 488 nm. Emission was detected between 493 and 531 nm for GFP. Per treatment and time point, 10 (Figure 3E) and 15 (Figure S3B) seedlings ( = biological replicates) were analyzed. For each seedling, 5-6 cells were measured for top and middle regions each ( = treated as technical replicates). Stacks of 57 to 90 images, covering the epidermal cell layer, were acquired with a 0.7 μm plane distance from the upper and the middle region of the hypocotyl. Imaging was performed with identical laser settings for all samples. Maximum projections of z stacks were analyzed with ImageJ (https://imagej.nih.gov/ij/) to measure the ratio between nuclear and cytoplasmic BZR1-GFP signals. A small area of fixed size covering approximately half of the nucleus was defined, and the mean fluorescence intensities were calculated within the nucleus and, for cytoplasmic values, in a field of identical size within the cytoplasm. The nuclear/cytoplasmic ratio was calculated for each individual cell.

### RNA extraction, cDNA synthesis, and qRT-PCR

RNA was extracted from three independent pools (n = 3) of 7-day-old seedlings grown at 20°C or 28°C in long day conditions. For shift experiments, 7-day-old seedlings were transferred to 28°C for the temperature treatment at ZT16. After 4 hr of cultivation (ZT20), samples were harvested. For continuous temperature treatment, seedlings were equally germinated at 20°C, and shifted to 28°C one day after germination, allowing further growth. RNA extraction was performed with an RNA purification kit (Macherey-Nagel) according to the manufacturer's protocols. Two microgram of total RNA was reverse-transcribed using the Revert Aid First Strand cDNA Synthesis Kit (Thermo Fisher Scientific). qRT-PCR analyses were performed using the ABsolute Blue QPCR SYBR Green low ROX Mix and gene-specific oligonucleotides (Key Resources Table). qRT-PCRs were performed on three biological replicates per time point using *At1g13320* as a reference gene [51]. Relative expression levels for each analyzed gene were calculated as $2^{\Delta Ct}$.

### Protoplast transient expression assay

*BZR1* was amplified from cDNA and cloned into the pENTR vector using the pENTR/D-Topo Cloning kit (Invitrogen). It was subsequently inserted into the expression vector pGWB406 (35S::-) by LR clonase recombination. A 2 kb fragment of the *PIF4* promoter was amplified from genomic DNA and cloned into the pNHL10 vector (*PIF4p:LUC*) using PstI and *NcoI* restriction enzymes.

*Arabidopsis* mesophyll protoplasts were isolated from Col-0 plants by the Tape-*Arabidopsis* Sandwich method [52]. After protoplast isolation, 10 μg total DNA was transfected as described in [53]. The *PIF4* promoter fused to firefly luciferase reporter gene was co-transfected with *35S:BZR1*. A CFP *(35S::CFP*) construct was co-transfected with *PIF4p:LUC* as a negative control. Transfected protoplasts were incubated overnight and luciferase expression was quantified next day. The firefly luciferase activities were normalized by β-glucuronidase (GUS) as an internal control of expression.

### ChIP-PCR

ChiP assays were performed as described previously [54]. Col-0 and *35S::BZR1-GFP* seedlings were germinated and grown for 7 days at 20°C in long day photoperiods. Half of the plates were transferred from 20°C to 28°C at ZT10 and the rest were left at 20°C. 4 g of material was harvested at ZT23 in the dark. The chromatin pellet was sonicated at 4°C with a Diagenode Bioruptor to achieve an average DNA fragment size of 0.3 to 0.8 kb. 1μl of anti-GFP (MBL International) and 10 μl of protein G coupled to magnetic beads (Invitrogen) were used for ChIP. DNA was purified using the MinElute Reaction CleanUp kit (QIAGEN). An aliquot of untreated sonicated chromatin was reverse cross-linked and used as input DNA control for PCR amplification (primers listed in the Key Resources Table). Relative fold-enrichment was calculated for each sample relative to their corresponding input and the wild-type. *PP2AA3* is represented as a negative control.

### Protein extraction and western blot

A total of 50 mg of plant material was harvested in 2 mL tubes and frozen in liquid nitrogen. Homogenization of the material was done using metal beads. RIPA buffer was added to each sample (200 μL buffer/50 mg plant material). Tubes were incubated in a shaker (200 rpm/4°C) for 15 min. After incubation, samples were centrifuged at maximum speed (14.000 rpm/ 4°C) for 20 min. The supernatant was collected and added to the protein loading buffer (4×). Tubes were incubated at 96°C for 10 min. A total of 30 μl sample was loaded on the SDS gel and subsequently transferred to a PVDF membrane.The western blot procedure was performed according to standard protocols using an anti-GFP antibody (Life technologies, A6455) according to to the manufacturer's specifications.

## QUANTIFICATION AND STATISTICAL ANALYSIS

Data visualization and statistical analyses of the data were performed using the software R (R Core Team, https://www.r-project.org/). Statistical analyses and plots were computed in R using built-in functions and the *ggplot2* package. Statistical information is specified in the figure captions.